Modeling hemodynamics in vascular networks using a geometrical multiscale approach: numerical aspects

Liesbeth Taelman[1], Joris Degroote[2], Pascal Verdonck[1], Jan Vierendeels[2], Patrick Segers[1]

[1]IBiTech-bioMMeda, Faculty of Engineering and Architecture, Ghent University

De Pintelaan 185, 9000 Gent, Belgium

[2]Department of Flow, Heat and Combustion Mechanics, Faculty of Engineering and Architecture, Ghent University

Sint-Pietersnieuwstraat 41, 9000 Gent, Belgium

Abbreviated title: Modeling hemodynamics using a geometrical multiscale approach

Corresponding author: Liesbeth Taelman

T: +32 9 332 41 98

Address: De Pintelaan 185, 9000 Gent, Belgium

Email address: Liesbeth.Taelman@UGent.be

Abstract

On the one hand the heterogeneity of the circulatory system requires the use of different models in its different compartments, featuring different assumptions on the spatial degrees of freedom. On the other hand, the mutual interactions between its compartments imply that these models should preferably not be considered separately. These requirements have led to the concept of *geometrical multiscale modeling*, where the main idea is to couple 3D models with reduced 1D and/or 0D models. As such detailed information on the flow field in a specific region of interest can be obtained while accounting for the global circulation. However, the combination of models with different mathematical features gives rise to many difficulties such as the assignment of boundary conditions at the interface between two models and the development of robust coupling algorithms, as the subproblems are usually solved in a partitioned way. This review aims to give an overview of the most important aspects concerning 3D-1D-0D coupled models. In addition, some applications are presented in order to illustrate the potentialities of these coupled models.

Key words: 3D-1D-0D models, dimensionally heterogeneous models, coupled problems, partitioned analysis, defective boundary conditions, absorbing boundary conditions.

1. Introduction

Cardiovascular disease (CVD) is the leading cause of death worldwide, accounting for one-third of all global deaths [44], and has a significant economic impact on the health care system, predominantly because of the escalating costs of advanced disease treatment. In 2010 CVD was responsible for 17% of national health expenditures in the United States [29]. Early detection and intervention of CVD can delay or prevent the symptoms from developing. It is therefore essential to have a profound understanding of cardiovascular (patho-) physiology to further improve diagnostic and therapeutic strategies and to tailor them to the individual patient rather than making clinical decisions based on population means. A powerful tool to gain insight into the hemodynamics and their relationship to vascular (dys)function is the numerical simulation of the blood circulation.

Modeling the fluid mechanics of the cardiovascular system is, however, a challenging task due to heterogeneity of the vascular tree in terms of geometrical and mechanical properties. Particularly, the diameters of the large arteries (> 10 mm), which carry the blood away from the heart, are considerably different from those of the capillaries (5-10 μm), where the smaller diameters and dense networks improve the actual exchange of water and chemicals between the blood and the tissues. Because of a decrease in characteristic length and velocity moving more distally in the arterial tree, viscous forces gain importance with respect to inertia forces. As a result, in the microcirculation, the viscous forces predominate the inertial forces and, in its most elementary form, a linear relation can be assumed between pressure and flow. Generally the blood flow is laminar. However, under conditions of high flow rate, particularly in the large arteries, laminar flow can be disrupted and become turbulent [38].
Another consequence of the decrease in characteristic length is the change in rheological behavior of the blood. In medium to large vessels, blood can be modeled as a continuum, obeying a Newtonian behavior [28] or, alternatively, incorporating the shear-thinning rheology [15, 53]. In the microcirculation, where the diameter of the blood vessels is comparable to the size of the red blood cells (8 μm), the blood cells are forced to migrate towards the center and move in single file, hereby strongly deforming (Fahraeus-Lindqvist effect). Consequently, the assumption that blood behaves as a fluid with uniform properties does no longer apply in smaller blood vessels and capillaries. Apart from the difference in geometrical properties, a significant diversity in mechanical properties of the vessel wall exists. The larger arteries are generally more elastic than the smaller ones. Deformations up to 10% of

the vessel radius are common in large arteries. This elasticity gives rise to the Windkessel effect (i.e. the distension of the large arteries during systole, functioning as a buffering reservoir for blood) [27, 68] and provides a passive mechanism for smoothing the pulsatile blood flow from the heart to the periphery. Although in most CFD simulations the wall is treated as rigid, it is important to consider the arterial wall behavior when one wants to simulate wave propagation in the arterial tree.

This heterogeneous composition of the cardiovascular system triggered the development of three classes of models (3D, 1D and 0D ones), featuring different assumptions on the spatial degrees of freedom. Three-dimensional (3D) models are usually applied when detailed information on the flow field (e.g. the wall shear stress distribution) is needed in a specific region. As the local blood flow is associated with the initiation and progression of certain cardiovascular diseases, such as atherosclerosis [14, 51], these 3D models provide a great contribution to the understanding of these diseases. Mathematically, the blood dynamics are described by the Navier-Stokes equations for incompressible fluids. These equations can be coupled to the equations of motion of the vessel wall to include the fluid-structure interaction (FSI). In [6, 17, 43] FSI simulations of the blood flow in cerebral aneurysms, a healthy aorta and Fontan patients are compared to rigid wall simulations, demonstrating the importance of including the flexible wall modeling, in particular with respect to the simulation of wall shear stress (which is overestimated in the rigid wall case of all three studies). Despite the advances made in computing power and numerical algorithms, the high computational cost and the intrinsic challenge of the FSI problem still restricts their use to a limited region, such as a bifurcation, the aortic arch or the examples listed above.
This limitation motivates the adoption of one-dimensional (1D) models, as they allow to compute the fluid dynamics in a large part of the arterial tree at a reasonable computational cost [23, 47]. The reduced model is obtained by assuming axial symmetry and by restricting the spatial variation of the

degrees of freedom to the axial direction. This restriction is justified, since the spectrum of wavelengths of the pressure waves generated by the heart is much longer than the diameter of the blood vessel [70]. Despite their lower level of accuracy, 1D models are an optimal tool to analyze arterial wave propagation. The spatial degrees of freedom of these models makes it, however, still unfeasible to model the whole capillary network with them.

A further simplification in the mathematical modeling is obtained by eliminating the variation in space. Zero-dimensional (0D) models, also called lumped parameter models, allow to describe the time evolution of the pressure and flow in a specific compartment of the circulatory system, like the heart or the capillary bed, although these models may also be used to describe the systemic or pulmonary circulation, or large parts of it.

Yet, the cardiovascular system is a closed system with a high level of interdependence. A global redistribution of the blood flow, which is a systemic feature, influences the hemodynamics in each vascular district, being a local feature (see for instance [13]). On the other hand, a local alteration, such as a vascular occlusion [9] or the presence of an aneurysm [11], can modify the systemic dynamics and give rise to compensatory mechanisms. For example in [2], it is shown that the presence of a stenosis in the carotid bifurcation does not imply a relevant reduction of the blood supply to the brain. Neglecting these interactions between local and global scales would therefore result in an inaccurate prediction of the fluid dynamics.

Thus, on the one hand the heterogeneity and extent of the circulatory system requires the use of different models in its different compartments. On the other hand, the mutual interactions between its compartments imply that these models should preferably not be considered separately. These requirements have led to the concept of *geometrical multiscale modeling* [7, 13, 18, 20, 24, 48], where the main idea is to couple dimensionally heterogeneous models, representing different physical compartments, to study the interaction between different geometrical scales. This approach applies 3D models only in those regions where a detailed knowledge of the flow field is needed, whereas 1D and 0D models are applied to represent the remaining part of the vascular tree. As such detailed information on the flow field in a specific region of interest can be obtained while at the same time accounting for the global circulation. Figure 1 conceptually illustrates a geometrical multiscale representation of the systemic circulation, where a 3D model of the left carotid bifurcation is included in a 1D model of the arterial tree and the microcirculation is described by three-element Windkessel models.

Several groups [37, 39, 45, 52, 59] have successfully coupled 3D models with 0D models, few of which take into account the fluid-structure interaction. As proposed by [35, 65], the prescription of a downstream vascular impedance at the boundaries of the 3D model, results in a more realistic incorporation of the wave reflections generated by the downstream vascular beds. However, the use of Womersley's linear wave theory to calculate the impedance restricts their application to time-periodic conditions. To extent their use to non-periodic conditions, an approach for prescribing lumped parameter outflow boundary conditions that accommodate transient phenomena has been presented in [66]. Few groups have studied the coupling of 3D-1D-0D models to consider the interactions between the local and systemic circulation [7, 10, 20, 40].

The choice between a 3D-1D-0D model or a 3D-0D model mainly depends on the objective of the application. Providing the reduced models are included to obtain proper boundary conditions at the artificial boundaries of a 3D model, both models can be used. However, often a 3D-0D model is preferred as it requires fewer parameters to determine and the ordinary differential equations describing the 0D models are easier to solve than the partial differential equations describing the 1D models. If, on the other hand, one wants to embed the 3D model into the (complete) circulatory system and study the interaction between global and local hemodynamics, a 3D-1D-0D coupled model should be used.

Despite the intuitiveness of multiscale modeling, the combination of models with different mathematical features, gives rise to many difficulties. The Navier–Stokes equations are nonlinear partial differential equations which can be parabolic, hyperbolic or elliptic (depending on the nature of the studied problem), while 1D models are described by hyperbolic partial differential equations, and 0D models are expressed in terms of a system of ordinary differential equations. This review aims to give an overview of the most important aspects concerning the geometrical multiscale approach and, in particular, the coupling between 3D and 1D models. In a first section, a description of the different models is given, followed by the mathematical and numerical issues related to their coupling. The next section is dedicated to the applicability of the geometrical multiscale approach to clinically relevant cases. Finally, some remarks are made on patient-specific modeling and the assessment of the quality of 3D-1D-0D coupled models representing the cardiovascular system.

2. Numerical Methods to Model the Fluid Dynamics at Different Scales

2.1 The zero-dimensional model

The main assumption in the modeling of the cardiovascular system as a Windkessel, is the hypothesis that the systemic pressure is homogeneous in space (Ω_{0D}). This assumption is justified if the wavelength of the pressure waves is sufficiently large compared to the dimensions of the system in which they propagate. As ageing and high blood pressure lead to stiffer arteries with an associated increase in wavelength, the arterial system - somewhat paradoxically - better resembles a Windkessel in these conditions [55].

Based on the analogy between hydraulic networks and electrical circuits, the two-element Windkessel model, introduced by Frank [27], consists of a parallel combination of a resistance R (representing the total peripheral resistance) and a compliance C (modeling the total arterial compliance). In the frequency domain, the input impedance of this model decreases from a value R at 0 Hz to a value close to zero at higher frequencies. This in contrast to the in vivo input impedance, which at higher frequencies corresponds to the characteristic impedance Z_0 of the system. To address this shortcoming, Westerhof [69] expanded the RC model to a three-element Windkessel model by placing the characteristic impedance in series with the RC model (see Figure 2). The differential equation describing the three-element Windkessel model is given by

$$\left(1+\frac{Z_0}{R}\right)Q + CZ_0\frac{dQ}{dt} = \frac{P}{R} + C\frac{dP}{dt} \qquad \text{in } \Omega_{0D} \qquad (2.1)$$

in which d/dt denotes the time derivative, Q the flow rate and P the spatially averaged pressure. In an attempt to further improve the accuracy of the input impedance, other more complex models have been developed, all of which can be expressed in terms of systems of ordinary differential equations [58].

Lumped parameter models can be used as well to model the functioning of the heart (i.e. the ventricular contraction). In [61], Suga et al. proposed a time-varying elastance model of the left ventricle. This model describes the ventricular pressure as a function of the change in ventricular volume and the ventricular elastance, which in turn is determined by three cardiac parameters: the maximal and minimal elastance and the time to maximum elastance. Many alternatives to this model are proposed such as the single-fiber model [3]. In this model the ventricular volume is determined by the change in fiber length and the ventricular pressure is related to the fiber stress. We refer to [58] for further details on lumped parameter models of the heart.

2.2 The one-dimensional model and 0D distributed model

In 1D models the arterial circulation is considered as a network of compliant vessels (Ω_{1D}) in which the flow is described by the one-dimensional equations for the conservation of mass and momentum. Several approaches have been developed to deduce and solve these 1D flow equations [58, 62]. Following the approach in [24], the blood vessels are assumed to be axisymmetric, having a fixed axis of symmetry. Furthermore, only radial displacements are taken into account and the pressure profile on each axial section is presumed constant. Finally, a particular velocity profile u_z is considered for which the axial components are assumed dominant. Under these assumptions, the flow equations are given by

$$\begin{aligned} \frac{\partial A}{\partial t} + \frac{\partial Q}{\partial z} = 0 \\ \frac{\partial Q}{\partial t} + \frac{\partial}{\partial z}\left(\frac{\alpha Q^2}{A}\right) + \frac{A}{\rho_f}\frac{\partial P}{\partial z} = -K_r \frac{Q}{A} \end{aligned} \qquad \text{in } \Omega_{1D} \qquad (2.2)$$

in which z denotes the axial coordinate and ρ_f the fluid density. The cross sectional area A, the flow rate Q and the pressure P are the unknowns in Eq (2.2). The friction parameter K_r and the momentum-flux correction coefficient α depend on the assumptions made regarding the shape of the velocity profile u_z. In general these coefficients are a function of the axial coordinate and time. However, most studies use a rather simplified velocity profile that can be written as

$$u_z(r, z, t) = \varphi(r)\bar{u}_z(z, t) \qquad (2.3)$$

where the shape function φ is radius dependent and the mean velocity $\bar{u}_z$ depends on the axial coordinate and the time. For these velocity profiles, the value of K_r and α reduces to a constant (e.g. $K_r = 8\pi\nu$ (ν denotes the kinematic viscosity) and $\alpha = 4/3$ correspond to a Poiseuille profile).

In order to close system (2.2) a constitutive law is needed, relating the vessel section A to the pressure P. Generally, circumferential stresses dominate radial and axial stresses and the inertia of the wall motion is neglected. With these restrictions, the wall mechanics reduce to an algebraic relation linking the pressure to the wall distension and consequently to the cross sectional area. This structural model corresponds to the so-called *independent rings* model [50]. More sophisticated models can be introduced by applying a differential law for the mechanics of the vessel wall.

Using an appropriate numerical technique (such as finite differences or the method of characteristics) and imposing continuity of (total) pressure and flow at the bifurcations, it is possible to compute the hemodynamics in the entire arterial tree.

Alternatively, the arterial tree can be treated as a transmission line [4, 56], based on the analogy between hydraulic networks and electrical circuits. In that case, the distributed model consists of a network of 0D models of which the parameters are defined using the Womersley theory. Constructing a transfer function between the pressures and flows at the inlet and the outlet of each segment, it is possible to compute the pressure and flow harmonics throughout the arterial tree in the frequency domain. Under the assumption of linearity, superposition of the different harmonics yields the final pressure and flow waves.

More details on the modeling of arterial wave propagation using 1D and 0D distributed models and the validation of the models against in vitro measurements can be found in [58, 62] and [1, 34] respectively.

2.3 The three-dimensional model

Consider the bounded domain Ω_{3D} representing a truncated artery (see for example Figure 2). The equations describing the unsteady Newtonian blood flow are given by the Navier-Stokes equations

$$\begin{gathered} \rho_f \frac{\partial \boldsymbol{u}}{\partial t} + \rho_f \boldsymbol{u}.\nabla \boldsymbol{u} - \nabla.\boldsymbol{\sigma}_f = \rho_f \boldsymbol{f} \\ \nabla.\boldsymbol{u} = 0 \end{gathered} \qquad \text{in } \Omega_{3D} \qquad (2.4)$$

with $\boldsymbol{u}$ the flow velocity and $\boldsymbol{f}$ the body forces acting on the blood per unit of mass. The Cauchy stress tensor $\boldsymbol{\sigma}_f$ is defined as

$$\boldsymbol{\sigma}_f = -p\boldsymbol{I} + \boldsymbol{\tau} \qquad (2.5)$$

with p the pressure, $\boldsymbol{I}$ the unit tensor and $\boldsymbol{\tau}$ the viscous stress tensor.

The prescription of boundary conditions is required to obtain a mathematically well posed problem. Typically, the velocity components (Dirichlet condition), the projection of the Cauchy stress tensor on the surface normal (Neumann condition) or a combination of both (Robin condition) are prescribed at the artificial boundaries Γ_i $(i = 1, \dots, n)$ and a no-slip condition is assumed at the physical arterial wall, denoted by Γ_w. The set of equations is discretized in space and time and solved iteratively.

The compliance of the model can be accounted for in fluid-structure interaction simulations, solving the flow and structural problem in a (strongly) coupled way. Several constitutive models have been devised to describe the mechanical dynamics of the arterial wall for 3D models, ranging from linear elastic and hyperelastic models to complex anisotropic models capturing the orientation of the collagen fibers, the dispersion in orientation and the mechanical behavior associated with the activation of smooth muscle cells. Reference [32] provides an overview of the current state of the art in constitutive modeling of the arterial wall behavior.

The interaction between the blood flow and the structure is enforced by imposing kinematic and dynamic equilibrium at the fluid-structure interface.

$$\begin{aligned} \boldsymbol{u} &= \frac{\partial \boldsymbol{\eta}}{\partial t} \\ \boldsymbol{\sigma}_f . \boldsymbol{n}_f &= -\boldsymbol{\sigma}_s . \boldsymbol{n}_s \end{aligned} \qquad on\ \Gamma_w \qquad (2.6)$$

In these equations $\boldsymbol{\eta}$ represents the wall displacement with respect to a reference position and $\boldsymbol{\sigma}_s$ the stress exerted by the structure on the fluid. $\boldsymbol{n}_f$ and $\boldsymbol{n}_s$ denote the unit normal vector pointing outwards from the fluid respectively the structural domain. A review on the numerical approaches used to solve the FSI problem and a discussion of the most important challenges can be found in [30, 33].

3. The geometrical multiscale approach – coupling issues

A common approach to handle dimensionally heterogeneous problems is to decompose the global domain into subdomains where the partitioning takes place at the interfaces between the models. Prescribing the continuity of some of the involved quantities at the coupling interfaces, the interaction between the subdomains is induced through the transfer of boundary data only. This way, a sequential solution of the 3D, 1D and/or 0D models can be used to obtain the global solution at each time step.

In case the 3D model is a rigid wall model, problems will occur when coupling the 3D model to a 1D model. As the compliance of the blood vessels is the driving mechanism of wave propagation in the 1D model, the coupling to a rigid 3D model will therefore, result in a discontinuous wall behavior at the interface, which in turn generates wave reflections and affects the numerical solution [49]. Compliance mismatch between 3D and 1D models can be prevented using fluid-structure interaction. FSI simulation is, however, not always relevant (providing the arterial wall deformation is limited and one is not interested in the stress distribution throughout the wall) and increases the computational cost significantly (as both the equations governing the flow and the arterial deformation need to be solved). To still allow coupling a 3D CFD simulation to a 1D model, one might introduce a simplified representation of the compliance of the 3D vessel at the interface with the 1D model [49]. The quantification of the parameters in these models is, however, a cumbersome task and unreliable results can be obtained if the quantification is incomplete [49].

3.1 Coupling 3D to 0D/1D models: options for boundary treatment

The numerical simulation of dimensionally heterogeneous problems implies the assignment of proper boundary conditions at the interface between two models. The choice of the transferred boundary data depends upon the underlying models and, in particular, upon the physical quantities for which some sense of conservation or continuity exists. The prescription of the continuity of mass flow rate at the coupling interface guarantees the conservation of mass. This boundary condition addresses the so-called *flow rate problem,* assigning a flow rate Q_i through each of the boundaries Γ_i $(i = 1, \dots, n)$ of the 3D domain.

$$\int_{\Gamma_i} \boldsymbol{u}.\boldsymbol{n}\ d\gamma = Q_i \qquad \text{on } \Gamma_i \qquad (3.1)$$

Due to the incompressibility of the fluid, the compatibility condition $\sum_{i=1}^{n} Q_i = 0$ must be fulfilled at each instant of time for the rigid CFD case. For FSI simulations, incorporating the compliance of the arteries, the difference between in- and outflow is buffered in the deforming fluid domain.

The second quantity for which continuity is enforced at the interface, is the spatially averaged pressure P_i.

$$\frac{1}{|\Gamma_i|}\int_{\Gamma_i} p\ d\gamma = P_i \qquad \text{on } \Gamma_i \qquad (3.2)$$

This condition in combination with the Navier-Stokes equations (2.4), is often referred to as the *mean pressure problem*. In [18] continuity of the spatially averaged total (static + dynamic) pressure is preferred above continuity of the spatially averaged static pressure, as for this case conditional stability of the iterations between the 3D and 1D FSI models is proved analytically [20]. Nevertheless, whenever the dynamic pressure is small compared to the static pressure, both the continuity of pressure and total pressure work equally well in terms of number of iterations between the 3D and 1D model and spurious wave reflections generated at the interface [18].

Still, the continuity of the flux and spatially averaged (total) pressure does not guarantee the continuity of cross sectional area at the interface. One can impose a zero stress boundary condition on the structure interface. However, in curved geometries, this might result in undesired wall deformations. On the other hand, clamping the vessel wall at the interface is unphysiological, since it generates spurious wave reflections at the interface. Alternatively, the continuity of the cross sectional area can be imposed as an additional coupling condition between two models [18, 21]. Yet, the prescription of the continuity of area combined with the continuity of mass flow rate and pressure, can provoke numerical instability due to a discrepancy in the structural models at the interface [19, 21]. Therefore, this condition is usually omitted [9, 19, 21].

From a mathematical point of view, the 3D Navier-Stokes problem requires the prescription of three scalars (such as the velocity components or the projection of the Cauchy stress tensor on the surface normal) at each point of the discretized boundaries. However, reduced 1D or 0D models provide only spatially averaged quantities. These conditions (referred to as *defective boundary conditions*) are insufficient to generate a well posed 3D problem, since its solution is not unique.
Different techniques have been devised to translate these defective boundary sets into mathematically sound boundary conditions for the Navier-Stokes problem, where we address 5 methods: (i) the prescription of an a priori selected flow profile, (ii) the do-nothing approach, (iii) a Lagrange multiplier approach, (iv) a minimization approach and (v) an extended variational approach.

(i) A common approach consists of prescribing an a priori selected velocity profile (flat, parabolic, Womersley) fitting the given flow rate, which has the drawback that the chosen velocity profile strongly affects the numerical solution in the 3D domain [67]. In order to reduce the sensitivity of the numerical solution in the zone of interest to the selected velocity profile, the computational domain is often extended (see for example [46, 67]).

(ii) In [31] a less perturbative strategy, the so-called *do-nothing approach*, was devised to address the mean pressure and flow rate problem using variational formulations. These formulations implicitly complete the defective data set with homogeneous Neumann conditions. Among all the possible physical solutions these formulations select the one that satisfies

$$\left(p - \nu \frac{\partial u_n}{\partial n}\right) = P_i, \qquad \frac{\partial \boldsymbol{u}_\tau}{\partial \boldsymbol{n}} = 0 \qquad \text{on } \Gamma_i \qquad (3.3)$$

with $u_n = \boldsymbol{u}.\boldsymbol{n}$ and $\boldsymbol{u}_\tau = \boldsymbol{u} - u_n\boldsymbol{n}$. In case the flow rates are prescribed at the boundaries, the pressures P_i present in these equations are unknown constants (in space). Consequently, the variational formulation devised to solve the flow rate problem, cannot be transformed into a fully equivalent formulation in terms of classical boundary conditions. Moreover, a non-standard functional space is used to handle the flow rate problem, which complicates the numerical implementation.

(iii) A different approach to solve the flow rate problem has therefore been proposed in [22, 63]. The basic idea is to consider Eq (3.1) as a set of constraints for the solution of the Navier-Stokes problem, rather than defective boundary conditions. Imposing of these constraints is achieved through the use of Lagrange multipliers λ_i $(i = 1, \dots, n)$. In terms of defective boundary data, the *Lagrange multiplier approach* is very similar to the do-nothing approach. The corresponding solution satisfies the additional boundary conditions

$$\left(p - \nu \frac{\partial u_n}{\partial n}\right) = \lambda_i, \qquad \frac{\partial \boldsymbol{u}_\tau}{\partial \boldsymbol{n}} = 0 \qquad \text{on } \Gamma_i \qquad (3.4)$$

in which the Lagrange multipliers λ_i replace the role of the unknown constants P_i of the do-nothing approach. The effectiveness of the proposed Lagrange multiplier methodology is illustrated in Figure 3, comparing the numerical solution of the flow in a rigid axisymmetric cylindrical pipe with the analytical one [64]. In case a steady flow rate is prescribed ($Q = 10^{-6}$ m³/s) the well-known Hagen-Poiseuille profile is recovered (see Figure 3, A). For a transient flow rate ($Q = \cos(2\pi t)\, 10^{-6}$ m³/s) an excellent agreement with the analytical Womersley solution is found (see Figure 3, B and C).

Using a standard functional space, the Lagrange multiplier formulation allows for a more straightforward numerical implementation. In [63] some numerical solution methods are proposed, based on the splitting of the computation of velocity and pressure and the computation of the Lagrange multipliers. This allows to perform the Navier-Stokes simulations with a standard solver, however, the iterative approach increases the computational cost significantly. Using an approximate reformulation of the problem (proposed in [64]), the computation becomes less expensive. On the other hand, a small error is introduced in the vicinity of the artificial boundaries.

(iv) While the do-nothing approach is not well-suited to solve the flow rate problem, the Lagrange multiplier approach cannot be applied to the mean pressure problem, since it provides unfeasible boundary conditions. In [25] a *minimization approach* is proposed, which allows to treat both problems efficiently and can therefore be used to solve problems where the two conditions are prescribed simultaneously. The approach is based on the minimization of a functional, quantified by the difference between the solution at the boundaries and the prescribed data.

Despite the fact that the previously mentioned methods (ii, iii and iv) were devised for rigid wall models, they can easily be extended to compliant models. Providing the flow and structural problem are solved separately, a rigid fluid problem in a 'frozen' domain is addressed at each FSI iteration. Consequently, the approaches described above can easily be applied. Solution strategies for the flow rate problem that allow for both a monolithic and partitioned FSI approach are developed in [26].

(v) A final method discussed here is based on an extended variational formulation for problems where fields can become discontinuous at some artificial internal boundary (regarded as the coupling interface) [9]. This approach is motivated by the discontinuities that arise in the velocity profiles at the interfaces due to the differences in underlying kinematics of the 3D and reduced models. The extended variational formulation allows for both a monolithic and partitioned solution of the 3D-1D coupled problem.

It is clear that all of the above described approaches provide relatively poor information at the coupling interfaces of the 3D-1D or 3D-0D models. As such, no reliable solutions must be expected in these regions.

3.2 Techniques to couple 3D and 1D models

In the following, some numerical techniques devised to solve 3D-1D coupled models are discussed. Remark that these techniques can also be used to couple 3D models with lumped parameter models, however, more efficient approaches (such as the *coupled multidomain method* [65]) can be applied there. The first strategy to handle geometrical multiscale models in an iterative way is based on an explicit approach [20]. In an explicit coupling, the flow rates Q_i $(i = 1, \dots, n)$ computed by the 3D solver are imposed as boundary conditions to the 1D models, which in turn compute the mean (total) pressures P_i $(i = 1, \dots, n)$ to be fed into the 3D model during the next time step. The 3D problem with imposed mean (total) pressures can be solved following the do-nothing approach or the minimization approach. Alternatively, the coupling conditions can be reversed, solving the 3D model with imposed flow rate resorting to the Lagrange multiplier approach or the minimization approach. Since only one iteration per time step is performed, the continuity of normal (total) stress and mass flow rate is not strictly preserved.

A straightforward approach to overcome this issue resorts to Dirichlet-to-Neumann (Gauss-Seidel) iterations with a relaxation procedure [9, 21]. A flow chart illustrating this approach is given in Figure 4. Each time step, coupling iterations between the 3D and 1D solver are performed until the pressure residuals fall below a prescribed tolerance ε. Fine-tuning of the relaxation parameter ω is, however, a time-consuming task and convergence of the algorithm is not guaranteed, especially when an elevated number of coupling interfaces are involved.

This concern led to the development of more robust iterative strong coupling techniques [40, 41]. The idea behind these techniques is to reinterpret the original coupled problem as an interface problem in terms of interface variables. This reformulation of the Dirichlet-to-Neumann problem allows to apply more sophisticated algorithms such as the Broyden-type methods or the Newton generalized minimal residual (GMRES) method. Another advantage of this approach is the flexibility concerning the type of boundary conditions imposed at the coupling interface. The chosen type of boundary condition on one side of the interface does not depend on the choice made on the other side of the interface.

4. Numerical examples and (clinical) applications

In this section, we present some applications of 3D-0D and 3D-1D-0D coupled models in hemodynamic simulations, in order to illustrate the potentialities of geometrical multiscale modeling.

A simple yet numerically most interesting case is the study of the propagation of a pressure pulse in a cylindrical blood vessel, see Figure 5 (left), where the propagation of a pressure pulse (10 mmHg, imposed during 3 ms) simulated with a full 3D FSI model is compared to the propagation obtained using a 3D-1D coupled model (interface at 5 cm). This clearly illustrates the potential of the 1D model as an absorbing boundary condition, eliminating spurious wave reflections at the outlets of the 3D model [20, 48]. Although this case is unphysiological in terms of geometry and boundary conditions, it is extremely useful for validation and to assess the characteristics of the coupling and, in particular, the reflections generated at the interface. A more quantitative comparison on the same case is given in Figure 5 (right), depicting the temporal evolution of the averaged pressure of the reference and the coupled solution at two different cross sections. The first section is located at 2.5 cm from the inlet and the second one at the

3D-1D interface. Apart from some small spurious reflections, a good agreement between both solutions is found.

The application of 3D-1D-0D models to clinically relevant cases, is mainly devoted to simulations in which the interactions between the global (arterial tree) and the local scales (specific arterial district) are of particular interest. In [13] the sensitivity of local hemodynamics to modifications in the heart inflow boundary condition is studied using a 3D-1D-0D coupled FSI model. Here, the functioning of the heart is represented by a prescribed flow rate (which in itself is a quite hard inlet boundary condition; coupling with a lumped parameter model of the heart might be the more flexible and physiologically correct option). In this study the heart rate (HR)is increased from 50 to 150 bpm to predict the effect of exercise on the local blood flow behavior in the carotid bifurcation using the model shown in Figure 1. In order to compare resting and exercise conditions, the inflow profile at the aortic root (taken from [60]) was scaled in time and flow rate such that the cardiovascular parameters depicted in Table 1 were retrieved. To obtain a total systemic resistance consistent with the prescribed cardiac output (CO) and mean pressure (MP), all terminal resistances were multiplied by the same scaling factor. Quantitative results are given in Figure 6, comparing the calculated flow at the inlet of the bifurcation and the oscillatory shear index (OSI) for the different heart rates considered. Although the shape of the imposed inlet profile was the same in all cases, the flow rate at the bifurcation is significantly affected by the HR, a non-trivial finding illustrating the relevance of multiscale modeling. For a low HR (50bpm) a small recirculation region is present at the carotid sinus with OSI values up to 0.4. This region enlarges for a HR of 70 bpm, whereas for higher HRs a ring pattern is formed containing higher OSI values close to 0.5. Regarding the mean wall shear stress (i.e. the WSS index integrated over the whole arterial wall) two observations can be made: (1) the mean WSS increases linearly with increasing CO and (2) the mean WSS is piecewise linear for HRs from 50 to 90 bpm and 90 to 150 bpm.

Another relevant application is the study of the influence of a pathological condition on the local and global hemodynamics. In [36], for instance, the effect of a stenosed coronary artery on the coronary flow and pressure is studied using a model that accounts for the interactions between the heart and the arterial system, rather than imposing "hard" boundary conditions (such as flows or predetermined flow distribution). It is demonstrated that the coronary flow remains unchanged up to 75% diameter reduction, which is a result matching clinical observations.
Apart from the analysis of alterations in the hemodynamic response, these studies also allow to evaluate whether the boundary conditions taken in a healthy case are still valid when simulating the pathological one. An example here is [11], where the sensitivity of the arterial pulse to the presence of an aneurysm in the internal carotid artery is studied by coupling a 3D FSI model of the carotid artery to a 1D model of the arterial tree. The hemodynamic quantities proximal to the aneurysm are the most perturbed and show larger fluctuations compared to the healthy case, indicating that boundary conditions applying to the healthy case cannot simply be transferred to the pathological case.

Other applications involve the simulation of cardiovascular interventions. In [37] for example, the reduction of the cardiac load is studied when comparing the pre-intervention and post-intervention hemodynamic conditions in an aorta with an aortic coarctation. In this quite advanced yet elegant study, a lumped parameter model of the heart is coupled to a 3D patient-specific model of an aorta with an aortic coarctation. The downstream circulation is modeled using three-element Windkessel models and the surgical procedure is simulated by applying surgical guidelines to connect the aorta proximal and distal to the coarctation. As the surgical resection entails a decrease of the arterial resistance, a reduced afterload and contractility of the left ventricle were obtained. The reduced pressure loss in the post-intervention case is clearly visible in Figure 7.

Other examples can be found in [5, 45], in which a multiscale model is applied to quantitatively compare hemodynamics after the treatment of single ventricle malformations.

From the previous examples it should be clear that a local alteration in a vascular district (such as a stenosis or an aneurysm) induces a redistribution of the global blood flow. This redistribution may, however, give rise to compensatory mechanisms to maintain arterial blood pressure and overall cardiovascular functioning within a narrow range of variation. Consequently, when simulating a medical intervention or pathological condition, some geometrical, mechanical and/or parameters of the coupled 0D models might require adjustment. With respect to this issue, a 3D-1D-0D model for the entire cardiovascular system has been extended with a 0D model of the homeostatic mechanisms corresponding to baroreflex actions in [12]. This self-regulating model allows to study the impact of baroreflex (dys)function on the local and global hemodynamics.

5. Final considerations

An issue that arises when applying the geometrical multiscale approach involves the correctness of the partitioning that divides the global domain into subdomains for which different kinematics are assumed. For instance, the length of the 3D model of the carotid artery in Figure 1 might affect the local and global flows predicted by the multiscale model. To avoid that a change in interface position significantly affects the solution of the coupled problem, a location needs to be determined for which the assumptions made on the spatial degrees of freedom are valid. This location depends on the solution of the problem and can thus not a priori be defined [8].

To assess the validity of the partitioning of a domain, a sensitivity analysis can be used [54] to determine the sensitivity of a given cost functional when the configuration of the coupled model is altered.

Providing the sensitivity of the solution is small, reliable results are obtained. The main advantage of this approach is that the analysis can be performed without changing the actual interface position [8].

When applying 3D-1D-0D coupled models for patient-specific modeling approaches, it is important to use a patient-specific geometry of the arterial tree (extracted from medical images) and to properly fit the mechanical and lumped parameters of the models to noninvasive measurements (e.g. MRI, Doppler,…). This is, however, a difficult and time-consuming task and is probably the biggest limitation to the use of dimensionally heterogeneous models in large-scale clinical studies [62].

In order to describe the entire systemic circulation, a model of the venous system and the heart should be included. Due to the presence of the valves, the noncircular cross sections and the highly nonlinear pressure-diameter relation in the venous system, this is a rather challenging task. Obviously, this also applies to closed loop models of the complete cardiovascular system, accounting for both the pulmonary and systemic circulation. Contributions in this direction are provided by [5, 12, 16, 42, 45].

In general, it can be stated that geometrical multiscale models allow to perform quantitative and qualitative studies on the interaction between local and global quantities in the cardiovascular system. These are indeed applications that are beyond the capabilities of stand-alone 3D, 1D and 0D models. Despite the number of applications of 3D-1D coupled models is still fairly limited, the strength of these models suggests they will provide an important contribution in the next step towards more realistic hemodynamic simulations. Some foreseen applications include the simulation of (surgical) treatments to study the alterations in local and global hemodynamics and the shape sensitivity analysis of a 3D geometry to optimize anastomosis procedures with respect to some hemodynamic quantities involving both scales.

This review paper is limited to geometrical multiscale models for cardiovascular hemodynamic research, and does not consider coupling with, for instance, cellular or subcellular models describing biological functions – which might interplay and interfere with the parameters of the 3D, 1D or 0D models described here. In addition to different geometrical scales, also different time scales need to be crossed and linked.

Acknowledgments

This research was funded by the Research Foundation - Flanders (FWO-Vlaanderen), project nr 3G008509. Joris Degroote gratefully acknowledges a post-doctoral fellowship of the Research Foundation - Flanders (FWO-Vlaanderen). The authors also would like to acknowledge Koen Van Canneyt for his support.

References

1. Alastruey, J., A. W. Khir, K. S. Matthys, P. Segers, S. J. Sherwin, et al. Pulse wave propagation in a model human arterial network: Assessment of 1-D visco-elastic simulations against in vitro measurements. J. Biomech. 44: 2250-2258, 2011.

2. Archie, J. P., R. W. Feldtman. Critical stenosis of the internal carotid-artery. Surgery 89: 67-72, 1981.

3. Arts, T., P. H. M. Bovendeerd, F. W. Prinzen, R. S. Reneman. Relation between left-ventricular cavity pressure and volume and systolic fiber stress and strain in the wall. Biophysical Journal 59: 93-102, 1991.

4. Avolio, A. P. Multi-branched model of the human arterial system. Med. Biol. Eng. Comput. 18: 709-718, 1980.

5. Baretta, A., C. Corsini, A. L. Marsden, I. E. Vignon-Clementel, T. Y. Hsia, et al. Respiratory effects on hemodynamics in patient-specific CFD models of the Fontan circulation under exercise conditions. Eur. J. Mech. B-Fluids 35: 61-69, 2012.

6. Bazilevs, Y., M. C. Hsu, Y. Zhang, W. Wang, X. Liang, et al. A fully-coupled fluid-structure interaction simulation of cerebral aneurysms. Computational Mechanics 46: 3-16, 2010.

7. Blanco, P. J., M. Discacciati, A. Quarteroni. Modeling dimensionally-heterogeneous problems: analysis, approximation and applications. Numerische Mathematik 119: 299-335, 2011.

8. Blanco, P. J., R. A. Feijoo. Sensitivity analysis in kinematically incompatible models. Computer Methods in Applied Mechanics and Engineering 198: 3287-3298, 2009.

9. Blanco, P. J., R. A. Feijoo, S. A. Urquiza. A unified variational approach for coupling 3D-1D models and its blood flow applications. Computer Methods in Applied Mechanics and Engineering 196: 4391-4410, 2007.

10. Blanco, P. J., M. R. Pivello, S. A. Urquiza, N. Albuquerque de Souza e Silva, R. A. Feijoo. Coupled models technology in multi-scale computational haemodynamics. International Journal of Biomedical Engineering and Technology 5: 132-156, 2011.

11. Blanco, P. J., M. R. Pivello, S. A. Urquiza, R. A. Feijoo. On the potentialities of 3D-1D coupled models in hemodynamics simulations. J. Biomech. 42: 919-930, 2009.

12. Blanco, P. J., P. R. Trenhago, L. G. Fernandes, R. A. Feijoo. On the integration of the baroreflex control mechanism in a heterogeneous model of the cardiovascular system. International Journal for Numerical Methods in Biomedical Engineering 28: 412-433, 2012.

13. Blanco, P. J., S. A. Urquiza, R. A. Feijoo. Assessing the influence of heart rate in local hemodynamics through coupled 3D-1D-0D models. International Journal for Numerical Methods in Biomedical Engineering 26: 890-903, 2010.

14. Caro, C. G., K. Parker. The effect of hemodynamic factors on the arterial wall. In Atherosclerosis-Biology and Clinical Science, ed. Olsson, A. G., Edinburgh: Churchill Livingstone,1987, 183-195 pp.

15. Carreau, P. J. Rheological equations from molecular network theories. Transactions of the Society of Rheology 16: 99-&, 1972.

16. Chow, K. W., C. C. Mak. A simple model for the two dimensional blood flow in the collapse of veins. J. Math. Biol. 52: 733-744, 2006.

17. Crosetto, P., P. Reymond, S. Deparis, D. Kontaxakis, N. Stergiopulos, A. Quarteroni. Fluid-structure interaction simulation of aortic blood flow. Computers & Fluids 43: 46-57, 2010.

18. de Moura, A. The geometrical multiscale modelling of the cardiovascular system: coupling 3D FSI and 1D models. PhD thesis. Politecnico di Milano, Milan. 2007. 136 pp.

19. de Moura, A., C. Vergara. Flow rate boundary conditions and multiscale modelling of the cardiovascular system in compliant domains. In Modelling in Medicine and Biology VI, Southampton: Wit Press/Computational Mechanics Publications,2005, 351-359 pp.

20. Formaggia, L., A. de Moura, F. Nobile. On the stability of the coupling of 3D and 1D fluid-structure interaction models for blood flow simulations. ESAIM-Mathematical Modelling and Numerical Analysis-Modelisation Mathematique Et Analyse Numerique 41: 743-769, 2007.

21. Formaggia, L., J. F. Gerbeau, F. Nobile, A. Quarteroni. On the coupling of 3D and 1D Navier-Stokes equations for flow problems in compliant vessels. Computer Methods in Applied Mechanics and Engineering 191: 561-582, 2001.

22. Formaggia, L., J. F. Gerbeau, F. Nobile, A. Quarteroni. Numerical treatment of defective boundary conditions for the Navier-Stokes equations. SIAM Journal on Numerical Analysis 40: 376-401, 2002.

23. Formaggia, L., F. Nobile, A. Quarteroni, A. Veneziani. Multiscale modelling of the circulatory system: a preliminary analysis. Computing and Visualization in Science 2: 75-83, 1999.

24. Formaggia, L., A. Veneziani. 2003. Reduced and multiscale models for the human cardiovascular system. In Lecture notes VKI Lecture Series 2003-07. Brussels

25. Formaggia, L., A. Veneziani, C. Vergara. A new approach to numerical solution of defective boundary value problems in incompressible fluid dynamics. SIAM Journal on Numerical Analysis 46: 2769-2794, 2008.

26. Formaggia, L., A. Veneziani, C. Vergara. Flow rate boundary problems for an incompressible fluid in deformable domains: Formulations and solution methods. Computer Methods in Applied Mechanics and Engineering 199: 677-688, 2010.

27. Frank, O. The basic shape of the arterial pulse - 1st treatise - mathematical-analysis. Journal of Molecular and Cellular Cardiology 22: 255-277, 1990.

28. Gijsen, F. J. H., E. Allanic, F. N. van de Vosse, J. D. Janssen. The influence of the non-Newtonian properties of blood on the flow in large arteries: unsteady flow in a 90 degrees curved tube. J. Biomech. 32: 705-713, 1999.

29. Heidenreich, P., J. Trogdon, O. Khavjou, J. Butler, K. Dracup, et al. Forecasting the future of cardiovascular disease in the United States: a policy statement from the American Heart Association. Circulation Research 123: 933-944, 2011.

30. Heil, M., A. L. Hazel. Fluid-structure interaction in internal physiological flows. Annual Review of Fluid Mechanics 43: 141-162, 2011.

31. Heywood, J. G., R. Rannacher, S. Turek. Artificial boundaries and flux and pressure conditions for the incompressible Navier-Stokes equations. International Journal for Numerical Methods in Fluids 22: 325-352, 1996.

32. Holzapfel, G. A., R. W. Ogden. Constitutive modelling of arteries. Proceedings of the Royal Society a-Mathematical Physical and Engineering Sciences 466: 1551-1596, 2010.

33. Hou, G. N., J. Wang, A. Layton. Numerical methods for fluid-structure interaction - a review. Communications in Computational Physics 12: 337-377, 2012.

34. Huberts, W., K. Van Canneyt, P. Segers, S. Eloot, J. H. M. Tordoir, et al. Experimental validation of a pulse wave propagation model for predicting hemodynamics after vascular access surgery. J. Biomech. 45: 1684-1691, 2012.

35. Johnson, D. A., U. P. Naik, A. N. Beris. Efficient implementation of the proper outlet flow conditions in blood flow simulations through asymmetric arterial bifurcations. International Journal for Numerical Methods in Fluids 66: 1383-1408, 2010.

36. Kim, H. J., I. E. Vignon-Clementel, J. S. Coogan, C. A. Figueroa, K. E. Jansen, C. A. Taylor. Patient-Specific Modeling of Blood Flow and Pressure in Human Coronary Arteries. Ann. Biomed. Eng. 38: 3195-3209, 2010.

37. Kim, H. J., I. E. Vignon-Clementel, C. A. Figueroa, J. F. LaDisa, K. E. Jansen, et al. On coupling a lumped parameter heart model and a three-dimensional finite element aorta model. Ann. Biomed. Eng. 37: 2153-2169, 2009.

38. Klabunde, R. E. Cardiovascular Physiology Concepts: Lippincott Williams & Wilkins. 2011. 256 pp.

39. Lagana, K., G. Dubini, F. Migliavacca, R. Pietrabissa, G. Pennati, et al. Multiscale modelling as a tool to prescribe realistic boundary conditions for the study of surgical procedures. Biorheology 39: 359-364, 2002.

40. Leiva, J. S., P. J. Blanco, G. C. Buscaglia. Iterative strong coupling of dimensionally heterogeneous models. International Journal for Numerical Methods in Engineering 81: 1558-1580, 2009.

41. Leiva, J. S., P. J. Blanco, G. C. Buscaglia. Partitioned analysis for dimensionally-heterogeneous hydraulic networks. Multiscale Modeling & Simulation 9: 872-903, 2011.

42. Liang, F. Y., S. Takagi, R. Himeno, H. Liu. Biomechanical characterization of ventricular-arterial coupling during aging: A multi-scale model study. J. Biomech. 42: 692-704, 2009.

43. Long, C. C., M. C. Hsu, Y. Bazilevs, J. A. Feinstein, A. L. Marsden. Fluid-structure interaction simulations of the Fontan procedure using variable wall properties. International Journal for Numerical Methods in Biomedical Engineering 28: 513-527, 2012.

44. Mendis, S., P. Puska, B. Norrving. 2011. Global Atlas on Cardiovascular Disease Prevention and Control, World Health Organization, Geneva

45. Migliavacca, F., R. Balossino, G. Pennati, G. Dubini, T. Y. Hsia, et al. Multiscale modelling in biofluidynamics: Application to reconstructive paediatric cardiac surgery. J. Biomech. 39: 1010-1020, 2006.

46. Moyle, K. R., L. Antiga, D. A. Steinman. Inlet conditions for image-based CFD models of the carotid bifurcation: Is it reasonable to assume fully developed flow? Journal of Biomechanical Engineering-Transactions of the Asme 128: 371-379, 2006.

47. Mynard, J. P., P. Nithiarasu. A 1D arterial blood flow model incorporating ventricular pressure, aortic valve and regional coronary flow using the locally conservative Galerkin (LCG) method. Communications in Numerical Methods in Engineering 24: 367-417, 2008.

48. Nobile, F. Coupling strategies for the numerical simulation of blood flow in deformable arteries by 3D and 1D models. Mathematical and Computer Modelling 49: 2152-2160, 2009.

49. Passerini, T., M. de Luca, L. Formaggia, A. Quarteroni, A. Veneziani. A 3D/1D geometrical multiscale model of cerebral vasculature. Journal of Engineering Mathematics 64: 319-330, 2009.

50. Perktold, K., G. Rappitsch. Mathematical modeling of local arterial flow and vessel mechanics. In Computational Methods for Fluid-Structure Interaction, Harlow: Longman Scientific & Technical,1994, 230-245 pp.

51. Perktold, K., G. Rappitsch. Mathematical modeling of arterial blood flow and correlation to atherosclerosis. Technology and Health Care 3: 139-151, 1995.

52. Quarteroni, A., A. Veneziani. Analysis of a geometrical multiscale model based on the coupling of ODEs and PDEs for blood flow simulations. Multiscale Modeling & Simulation 1: 173-195, 2003.

53. Quemada, D. Rheology of concentrated disperse systems III. General features of the proposed non-Newtonian model. Comparison with experimental data. Rheol. Acta 17: 643-653, 1978.

54. Rousselet, B., E. J. Haug. Design sensitivity analysis in structural mechanics. Effects of shape variation. Journal of Structural Mechanics 10: 273-310, 1982.

55. Segers, P., E. R. Rietzschel, M. L. De Buyzere, S. J. Vermeersch, D. De Bacquer, et al. Noninvasive (input) impedance, pulse wave velocity, and wave reflection in healthy middle-aged men and women. Hypertension 49: 1248-1255, 2007.

56. Segers, P., N. Stergiopulos, P. Verdonck, R. Verhoeven. Assessment of distributed arterial network models. Med. Biol. Eng. Comput. 35: 729-736, 1997.

57. Seifter, J., A. Ratner, D. Sloane. Concepts in medical physiology. Philadelphia: Lippincott Williams & Wilkins. 2005.

58. Shi, Y. B., P. Lawford, R. Hose. Review of Zero-D and 1-D Models of Blood Flow in the Cardiovascular System. Biomedical Engineering Online 10: 38, 2011.

59. Shim, E. B., R. D. Kamm, T. Heldt, R. G. Mark. Numerical analysis of blood flow through a stenosed artery using a coupled multiscale simulation method. In Computers in Cardiology 2000, Vol 27, New York: IEEE,2000, 219-222 pp.

60. Spencer, M. P., A. B. Denison. The square-wave electromagnetic flowmeter - theory of operation and design of magnetic probes for clinical and experimental applications. Ire Transactions on Medical Electronics 6: 220-228, 1959.

61. Suga, H., K. Sagawa, A. A. Shoukas. Load independence of the instantaneaous pressure-volume ratio of the canine left ventricle and effects of epinephrine and heart rate on the ratio. Circulation Research 32: 314-322, 1973.

62. van de Vosse, F. N., N. Stergiopulos. Pulse Wave Propagation in the Arterial Tree. Annual Review of Fluid Mechanics 43: 467-499, 2010.

63. Veneziani, A., C. Vergara. Flow rate defective boundary conditions in haemodynamics simulations. International Journal for Numerical Methods in Fluids 47: 803-816, 2005.

64. Veneziani, A., C. Vergara. An approximate method for solving incompressible Navier-Stokes problems with flow rate conditions. Computer Methods in Applied Mechanics and Engineering 196: 1685-1700, 2007.

65. Vignon-Clementel, I. E., C. A. Figueroa, K. E. Jansen, C. A. Taylor. Outflow boundary conditions for three-dimensional finite element modeling of blood flow and pressure in arteries. Computer Methods in Applied Mechanics and Engineering 195: 3776-3796, 2006.

66. Vignon-Clementel, I. E., C. A. Figueroa, K. E. Jansen, C. A. Taylor. Outflow boundary conditions for 3D simulations of non-periodic blood flow and pressure fields in deformable arteries. Comput. Methods Biomech. Biomed. Eng. 13: 625-640, 2010.

67. Wake, A. K., J. N. Oshinski, A. R. Tannenbaum, D. P. Giddens. Choice of In Vivo Versus Idealized Velocity Boundary Conditions Influences Physiologically Relevant Flow Patterns in a Subject-Specific Simulation of Flow in the Human Carotid Bifurcation. Journal of Biomechanical Engineering-Transactions of the Asme 131: 8, 2009.

68. Westerhof, N., F. Bosman, C. J. Devries, A. Noordergraaf. Analog studies of human systemic arterial tree. J. Biomech. 2: 121-134, 1969.

69. Westerhof, N., G. Elzinga, P. Sipkema. Artificial arterial system for pumping hearts. Journal of Applied Physiology 31: 776-781, 1971.

70. Westerhof.N, F. Bosman, C. J. Devries, Noorderg.A. Analog studies of human systemic arterial tree. J. Biomech. 2: 121-134, 1969.

List of tables and figures

Figure 6: Flow rate at the inlet of the common carotid and OSI index as a function of heart rate. These results were obtained using the model depicted in Figure 1. Figure taken with the permission from Blanco (2010) [13].

Figure 7: (left) Lumped parameter models coupled to the 3D model of the aorta with an aortic coarctation. (right) Pressure contours (mmHg) in the aorta at three diffent times for the case of pre-intervention and post-intervention. Figure taken with the permission from Taylor (2009) [37].

Table 1: Cardiovascular parameters (heart rate HR, cardiac output CO, systole diastole ratio S/D and mean pressure MP) for the comparison of hemodynamic response at rest and during exercise. These data have been taken from [57].

HR (bpm)	CO (l/min)	S/D	MP (mmHg)
50	5	0.5	100
70	10	0.65	108
90	15	0.8	115
120	20	0.9	122
150	25	1.05	130

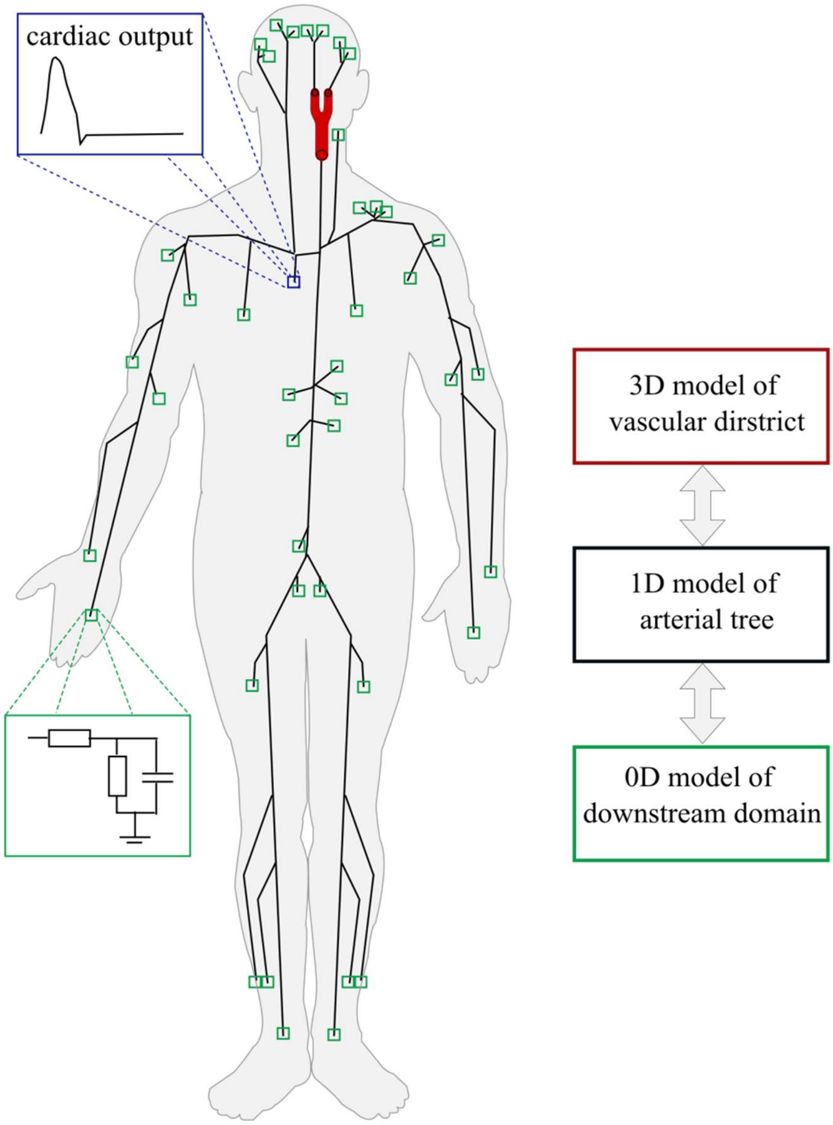

Figure 1: Geometrical multiscale model of the circulatory system, including a detailed model of the carotid bifurcation and Windkessel models to represent the downstream circulation.

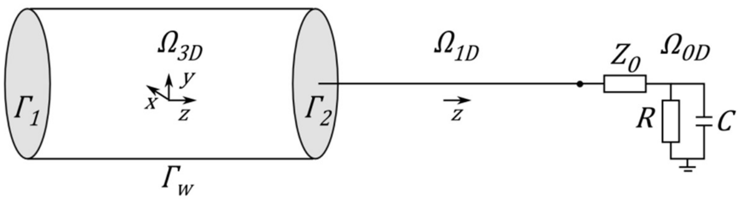

Figure 2: A simple 3D-1D-0D model, consisting of a cylindrical artery coupled to a 1D domain and a three-element Windkessel model.

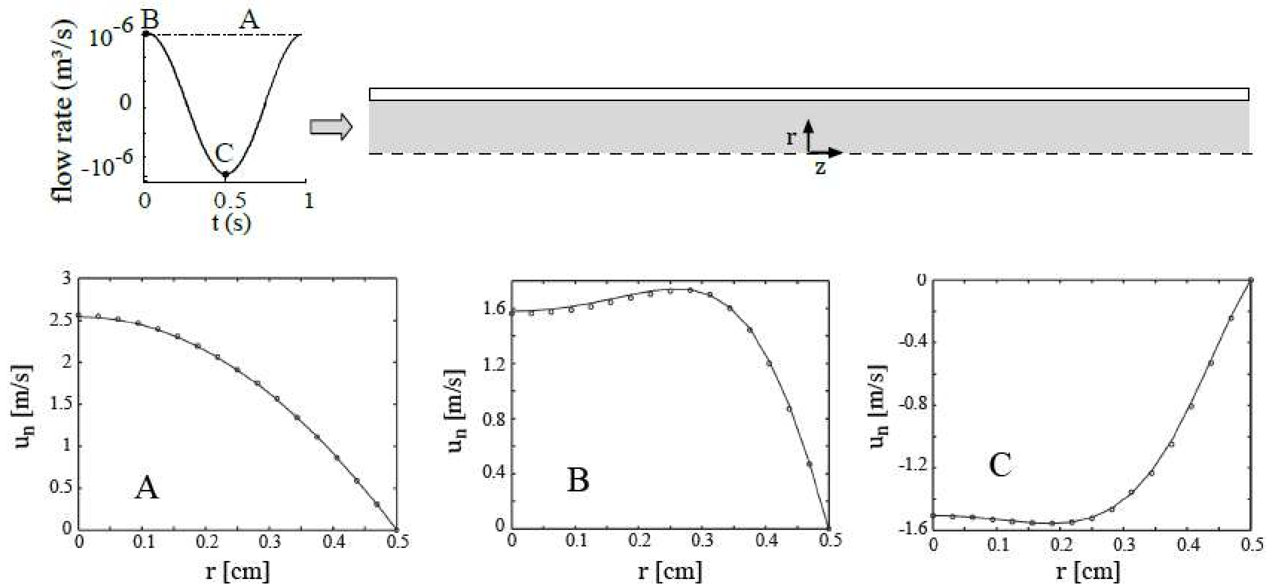

Figure 3: Comparison of the axial velocity profile ($\boldsymbol{u_n}$) in a rigid axisymmetric cylindrical pipe, obtained analytically and using the Lagrange multiplier approach. The results are shown for both, a steady inflow condition (A) and a periodic flow condition, (B) at the beginning of the period and (C) halfway the period. The markers refer to the numerical solution, the line to the analytical one. Figure reproduced with the permission from Veneziani (2007) [64].

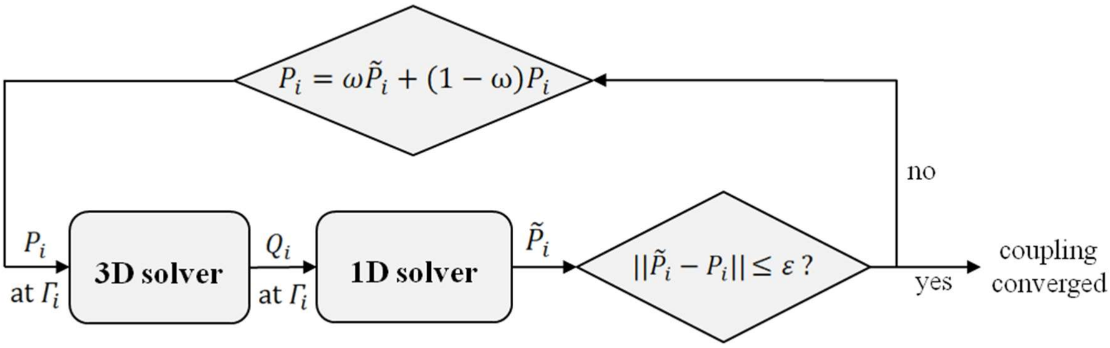

Figure 4: Flow chart illustrating Gauss-Seidel iterations with a relaxation procedure between a 3D and 1D flow solver.

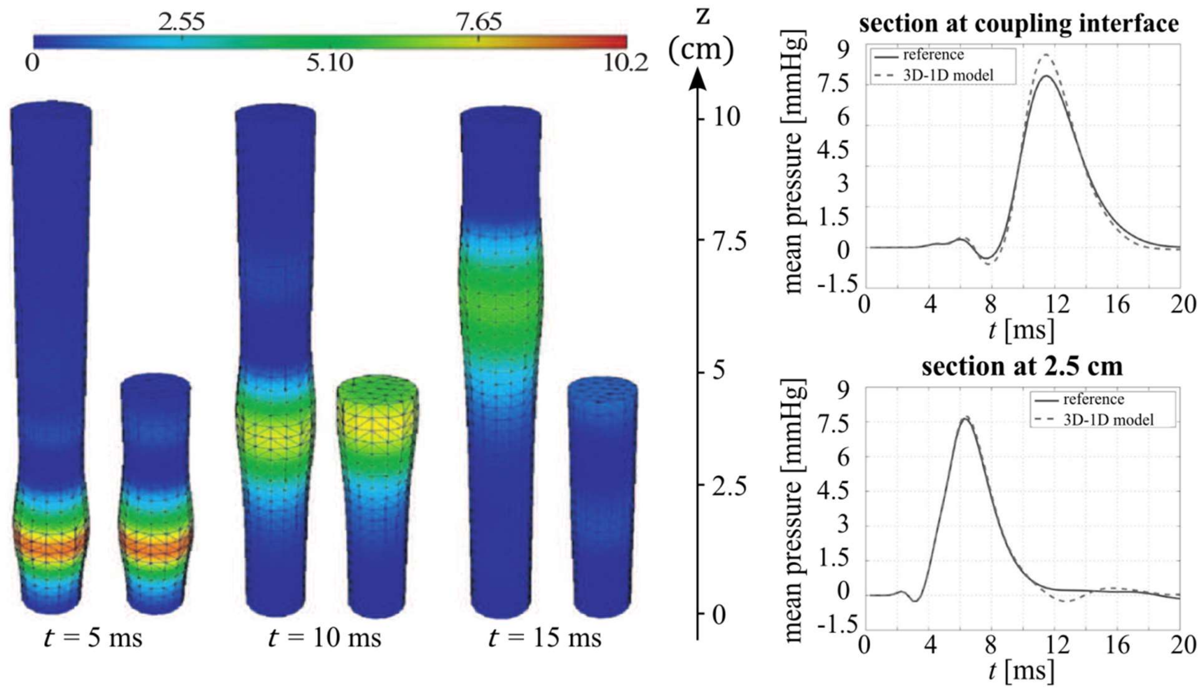

Figure 5: (left) Comparison between the pressure contours (mmHg) at three different times, obtained using a fully 3D model and a 3D-1D coupled model of which the interface is located halfway the flexible tube. (right) Comparison between the averaged pressure evolution at two different sections (top) 2.5 cm from the inlet and (bottom) at the coupling interface. Figure reproduced with the permission from Nobile (2009) [48].

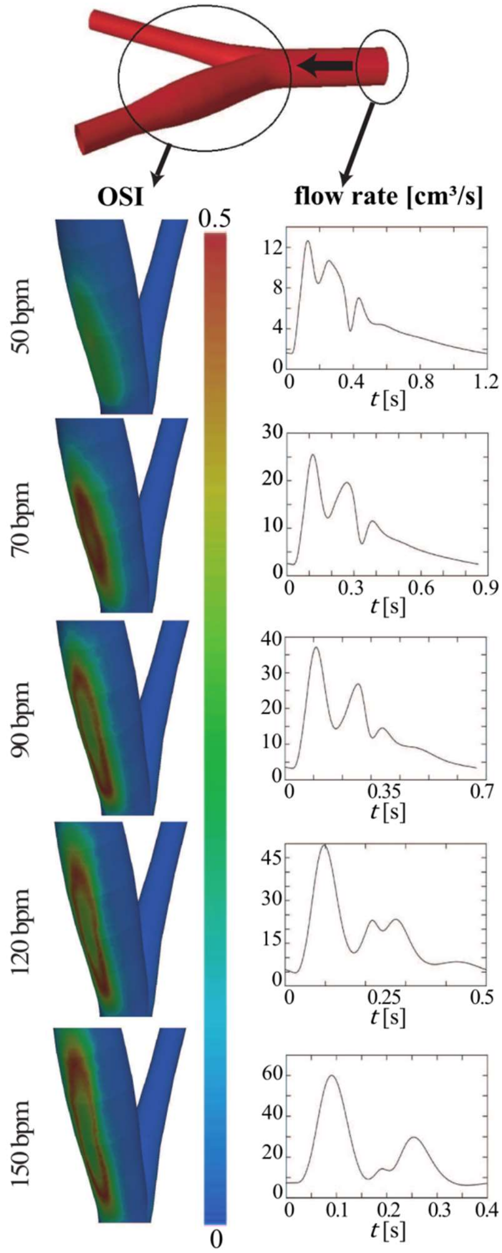

Figure 6: Flow rate at the inlet of the common carotid and OSI index as a function of heart rate. These results were obtained using the model depicted in Figure 1. Figure taken with the permission from Blanco (2010) [13].

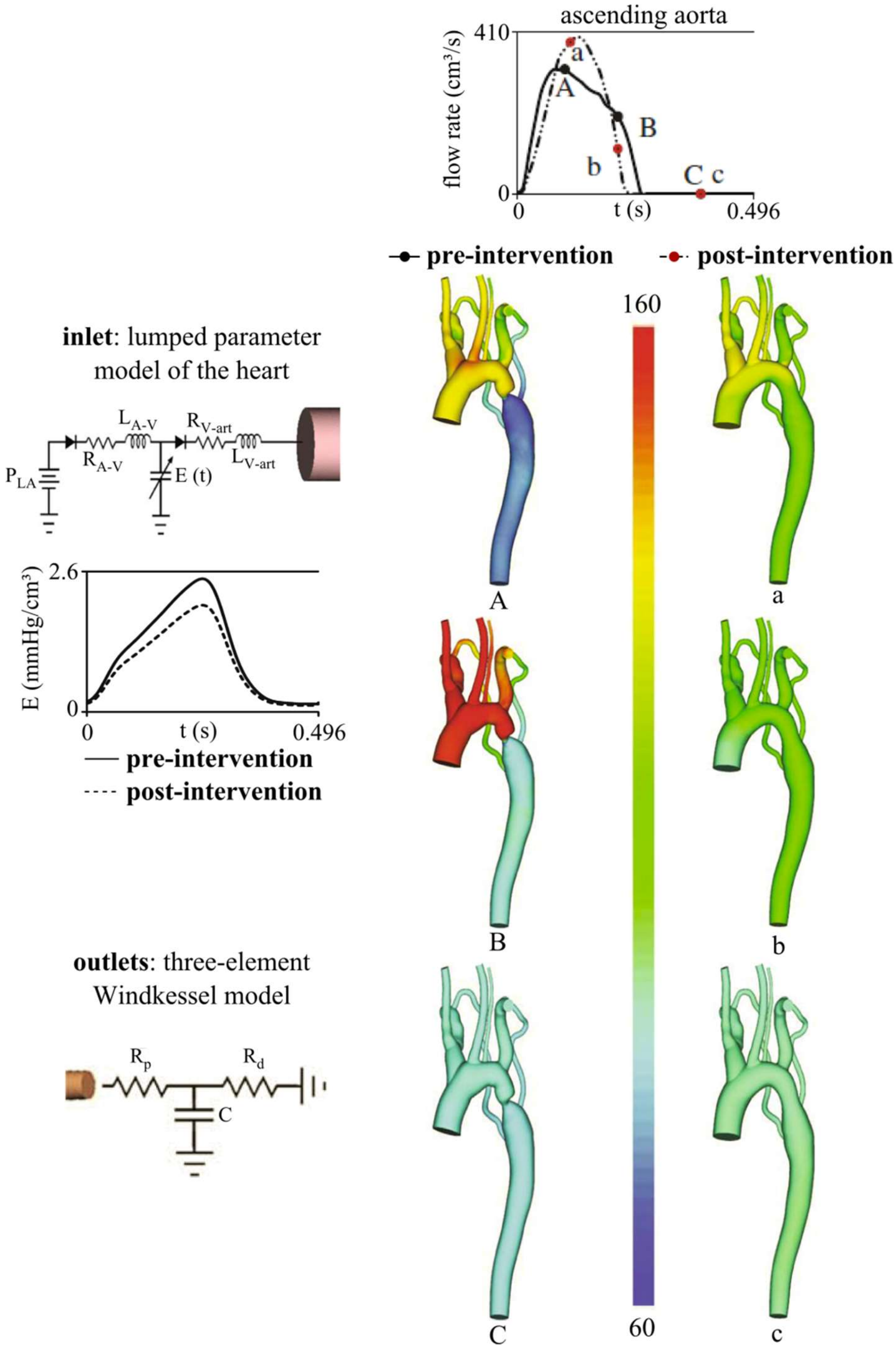

Figure 7: (left) Lumped parameter models coupled to the 3D model of the aorta with an aortic coarctation. (right) Pressure contours (mmHg) in the aorta at three diffent times for the case of pre-intervention and post-intervention. Figure taken with the permission from Taylor (2009) [37].